An Investigation of the Mechanism on Interfacial Charge Transformation of the TiB2/Cu Composites Studied by the First Principles

Yao Shu (shuyao_jack@2008.sina.com)
Guangdong Academy of Sciences https://orcid.org/0000-0001-8847-0549
Juan Wang
Guangdong Academy of Sciences
Yongnan Xiong
Guangdong Academy of Sciences
Xing Luo
Guangdong Academy of Sciences
Jiazhen He
Guangdong Academy of Sciences
Cuicui Yin
Guangdong Academy of Sciences
Fei Gao
Nanchang University
Shaowen Zhang
Beijing Institute of Technology
Kaihong Zheng
Guangdong Academy of Sciences
Fuxing Yin
Guangdong Academy of Sciences
Fusheng Pan
Guangdong Academy of Sciences

Research Article

Keywords: The first principles, Charge communications, Bond length, TiB2/Cu matrix composites

Posted Date: December 3rd, 2021

DOI: https://doi.org/10.21203/rs.3.rs-1125795/v1

An Investigation of the Mechanism on Interfacial Charge Transformation of the TiB_2/Cu Composites Studied by the First Principles

Yao Shu[a,b ǂ*], Juan Wang[a,b ǂ], Yongnan Xiong[a,b], Xing Luo[a,b], Jiazhen He[a,b], Cuicui Yin[a,b], Fei Gao[c], Shaowen,Zhang[d*], Kaihong Zheng[a,b*], Fuxing Yin[a,b], Fusheng Pan[a,b]

Abstract

The charge communications have been widely existed in the metal materials when they are under the processing, the modeling and the failing. We studied the interfacial charge transformation of the TiB_2/Cu composites via the first principles method. The layer thickness was predicted by the interfacial charge communications performed on the regions of the TiB_2/Cu interfaces. The layer thickness of the Ti-terminated (TT)TiB_2/Cu were predicted longer than those of the B-terminated(BT) TiB_2/Cu and contrasting with their average vales as 0.75 (nm) and 0.65 (nm), respectively. The Mulliken population was applied to investigate the bond length, bond population and charge transformation of the six TiB_2/Cu models. The Ti-Cu bond was only detected in TT-HCP interfaces among the all TT-TiB_2/Cu models, which was further confirmed that the metallic bond of the Ti-Cu with the bond length and population as 2.5 Å and 0.22, respectively. Nevertheless, the B-Cu bond were detected in all BT-TiB_2/Cu models, and the bond length and population higher than those of B-Cu bond in chemical complexes. The 5 atomic layers were involved in quantitative analyses of the interfacial charge transformation. The results indicate that the charges lost by interfacial Ti atom were inequivalent obtained by Cu and B atoms which nearby the interfacial Ti atoms of the TT-TiB_2/Cu. Comparing with the BT-TiB_2/Cu models, the charges acquired by the interfacial B atom were most from the Ti and less from the Cu atoms surrounded the interfacial B atoms.

Key word: The first principles, Charge communications, Bond length, TiB_2/Cu matrix composites

ǂ *represent the authors who have the same contributions for this work.*

1 Introduction

Copper metals have been widely applied into the electronic technology, transportation and aerospace fields due to its high electrical conductivity and premium ductility[1-3]. However, owing to the lower hardness and strength of the pure copper metals, the further applications of the copper metals are limited. Therefore, the copper alloy and copper matrix composites (CMCs) were designed to enhance the hardness and strength properties of the copper metals. Though, the copper alloy owns the better properties, the hardness while the ductility are still the conflict of not settled[4-7]. However, due to the reinforcements introduced into the copper metals, the hardness and strength of the copper matrix have been apparently enhanced. Therefore, CMCs have been widely utilized into the electronic technology, transportation and aerospace fields[8-11].

Due to the wildly application of the CMCs, the reinforcements have been verified to be the key factors for enhancing the hardness and strength of the CMCs. The reinforcements, however, are mainly classified as the carbide (B_4C, TiC, and WC)[12-14], the oxide (Al_2O_3, ZrO_2)[15,16] and the ceramic (Si_3N_4, AlN) [17,18] and which had been already applied into CMCs for years. Nevertheless, many theoretical studies have been investigated in interfacial electronic properties of the CMCs via the first principles studies, such as Al_2O_3/Cu[19], TiC/Cu[20], WC/Cu[21] ,ZrC[22] and TiB_2/Cu[23] composites. Although, these investigations are mainly focused on interfacial stabilities, electronic properties and interfacial ultimate tensile stresses, the quantum interfacial charge transformations of the CMCs were less to be considered. Therefore, the influence of interfacial stabilities specifically with the charge transformation of the interfacial atoms were not further discussed.

As is known to all, the charge communications have widely existed in biomolecules[24], organic electronic devices[25], semiconductors[26], super-molecules[27], catalysts[28], ceramics[29], metals[30], polymers[31] and so on. The properties of these materials are deeply affected and relayed on the charge communications when they syntheses, processed, decomposition and shaped.

In this essay we are concerning about the relationships between the charge transformations of the interfacial atoms and the interfacial stabilities. The interfacial stabilities, electronic properties and ultimate tensile stress of the TiB_2/Cu have been studied in previous works. Therefore, we have taken the interfacial charge transformations into account to investigate the influences of the charge transformation vs. the interfacial stabilities of the TiB_2/Cu.

2 Computational models and Methodology details

TiB_2/Cu interfacial models were constructed via the TiB_2 (0001)[32,33] and Cu (111)[34] surface, due to their low surface energies. In addition, we chosen three stacking ways of the Cu and two terminated atoms (Ti-terminated and B-terminated) of the TiB_2 to construct the TiB_2/Cu composites models. The three stacking sequences were considered for the Cu respective as "HCP", "MT" and "OT". In specific, the "HCP" stacking refers to the interfacial Cu atoms are on-top the first layer of TiB_2 atoms, "MT" stacking refers to the interfacial Cu atoms reside atop the midpoint of the atomic connection of the first layer of TiB_2 atoms and "OT" stacking means the interfacial Cu atoms reside atop the TiB_2 second layer atoms. Namely, there were six TiB_2(0001)/Cu(111) interfacial models generated for theoretical investigations. Therefore, six TiB_2/Cu interfacial models are shown in **Fig. 1**, and they are labeled as TT-HCP, TT-MT, TT-OT, BT-HCP, BT-MT and BT-OT respectively. In order to eliminate the interactions between the surface atoms, a 15 Å vacuum layer was added along z directions for each surface.

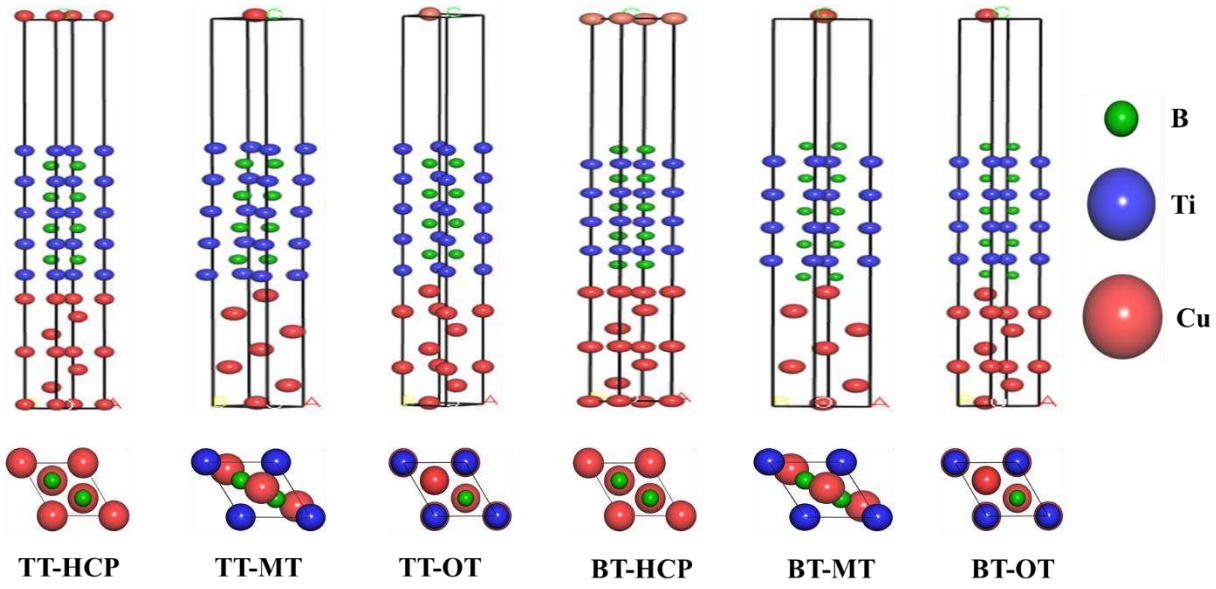

Fig. 1 The Ti-terminated (TT) and B-terminated(BT)-TiB_2(0001)/Cu(111) interfacial models. Above graphs are side view of the six TiB_2(0001)/Cu(111) interfacial models while the below are top view of the TiB_2(0001)/Cu(111) interfacial models. The green, blue and red balls are represent the B, Ti and Cu atoms, respectively.

All calculations calculated via the first principles method to TiB_2/Cu interfacial models under the periodic boundary conditions and plane wave basis set of the Cambridge Serial Total Energy Package (CASTEP) Code[35, 36]. The Perdew-Burker-Enzerhof (PBE) functional generalized gradient approximation (GGA) [37]were deal with the exchange-correlation interactions in the all

calculations. The Brillouin zone was sampled with the Monkhorst-Pack k-point grid[38] 11×11×1 for all TiB_2/Cu interfacial models, Cu(111) slab and TiB_2 (0001) slab, respectively. The atoms of the TiB_2/Cu were relaxed for acquiring the ground state by Broyden-Fletcher-Goldfarb-Shanno (BFGS) algorithm[39]. Nevertheless, the total energy tolerance, maximum force tolerance and maximal displacement calculating convergent details were applied as 1.0×10^{-5} eV/atom, 0.03 eV/Å and 1.0×10^{-5} Å, respectively. In addition, 500 eV was chosen as the cut-off energy for the plane wave as the expansion in reciprocal space. In order to calculate the electronic properties of the interfacial atoms, the $3d^{10}4s^1$, $3s^23p^63d^24s^2$, and $2s^22p^1$ valence electron configurations were applied to Cu, Ti and B atoms respectively. The total atoms for TT-TiB_2/Cu, Cu (111) slab and TiB(0001) slab are 20 (21 for BT- TiB2/Cu),7 and 13 (14 for BT-TiB_2(0001) slab), respectively.

3 Results and discussions

3.1 The interfacial thickness of the TiB_2(0001)/Cu(111).

The interfacial thickness is not referring to the distance of the interfacial atoms, but the range influenced by atomic electrons of the heterogeneous interface. Therefore, in this section, the PDOS

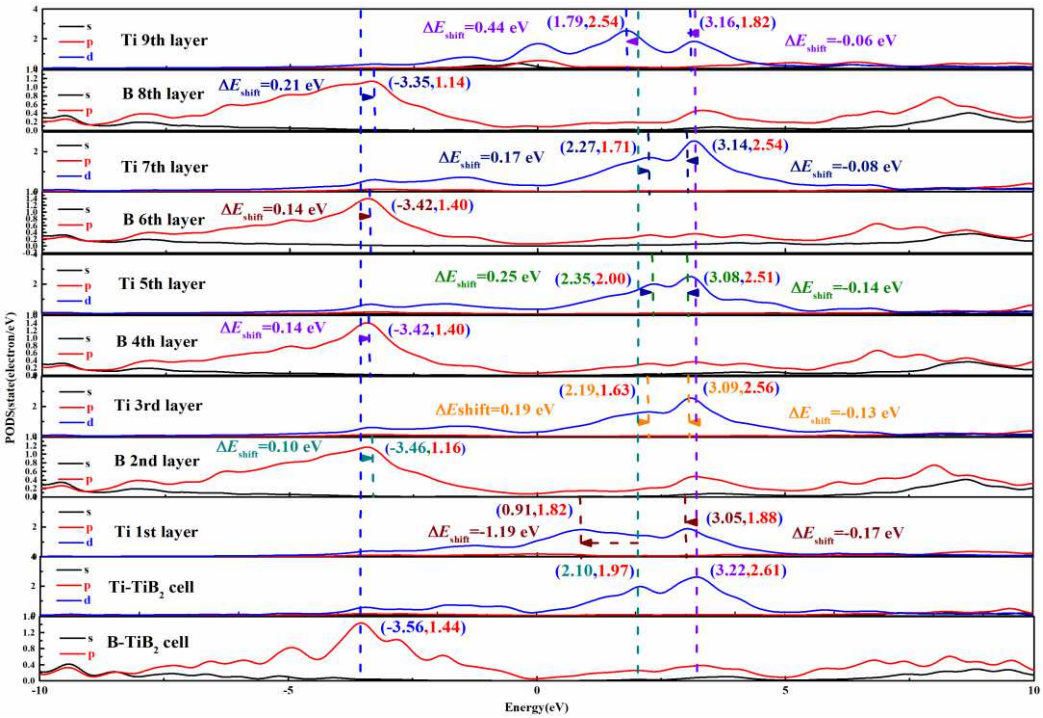

(a)

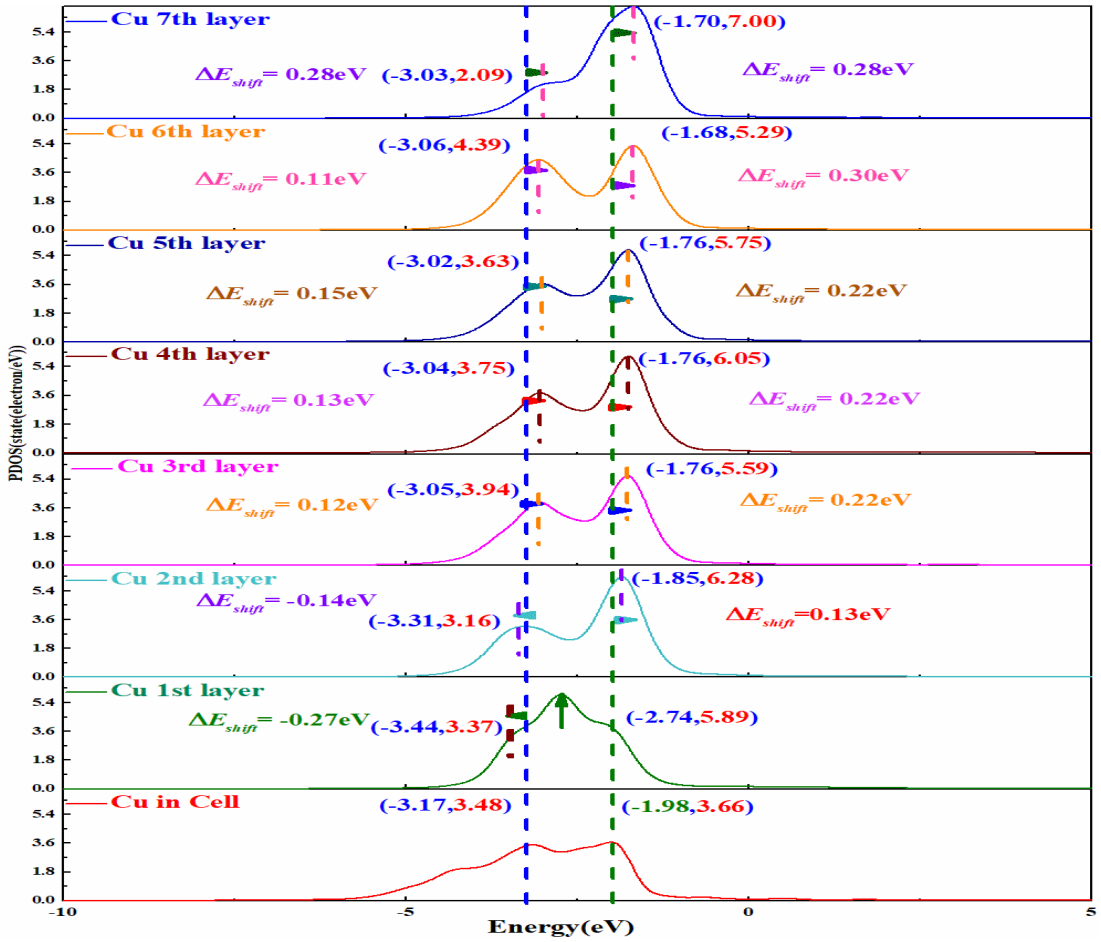

(b)

Fig. 2 The PDOS of B,Ti and Cu atoms in TiB_2(0001)/Cu(111), TiB_2 cell and Cu cell, respectively: **(a)** the PDOS of the Ti,B atoms in TT-HCP *vs.* those in TiB_2 cell, **(b)** the PDOS of the Cu in TT-HCP *vs.* those in Cu cell.

of the Ti, B and Cu atoms in TiB_2(0001)/Cu(111), TiB_2 cell and Cu cell are applied to confirm the interfacial thickness via the micro electron interactions. Taking TT-HCP for instance, the curves of the PDOS of Ti-*d* and B-*p* in TiB_2 cell are different with those of the 1st Ti and the 2nd B atoms of the TiB_2(0001)/Cu(111) in **Fig. 2 (a)**. Namely, the curve shape of the PDOS of the 1st Ti and the 2nd B atoms in TT-HCP are obviously changed not only to the intensity of the peak formations but also to the coordinate locations. Namely, the two peaks in the 1st Ti-*d* PDOS curves have -1.19 eV and -0.17 eV energy shifts and with 0.15 *e*/eV and 0.73 *e*/eV electron densities decreases contrasting to those of the Ti-*d* electrons in TiB_2 cell. Moreover, the curve of the PDOS of the 2nd B-*p* are also quite different with those of the interior B-*p* in TiB_2 cell, which imply that the electrons of the 2nd B-*p* orbit also indirectly influenced by the electrons of the *d* orbit of the interfacial Cu atoms.

Nevertheless, the electrons of the 3rd Ti-*d* and the 4th B-*p* orbit have less changes than those of 5th Ti, 6th B and 7th Ti interior atoms. The curves of the PDOS of the 8th B-*p* and the 9th Ti-*d* for TT-HCP are also different with those of the interior B-*p* and Ti-*d* in TT-HCP and TiB_2 cell, owing to the free electrons un-localized in the 15 Å vacuums region. Herein, it can be predicted that three atomic layers of the TiB_2 in TiB_2(0001)/Cu(111) are confirmed by the curves of PDOS for the partial layer thickness of the TiB_2(0001)/Cu(111).

On the other hand, the curves of the PDOS of the Cu-*d* in TT-HCP and Cu cell are displayed in **Fig. 2 (b)**. It can be noted that the two peaks located at -3.17 eV and -1.98 eV with the respective electron density states 3.48 *e*/eV and 3.66 *e*/eV for the PDOS of the Cu-*d* curves in Cu cell. The curve of the PDOS of the Cu-*d* in TiB_2(0001)/Cu(111) are distinct with those in Cu cell. Namely, the curve of

$$\Delta l = l_{TiB_2(z)} + l_{Cu(z)} \quad \textbf{(1)}$$

Table 1. The calculated interfacial thickness of TiB_2(0001)/Cu(111) (nm)

The possible interface of the TiB_2(0001)/Cu(111)						
Entry	TT-HCP	TT-MT	TT-OT	BT-HCP	BT-MT	BT-OT
Δl	0.757	0.716	0.717	0.657	0.657	0.702

the 1st PDOS of Cu-*d* in TiB_2/Cu has an obvious peak at -2.74 eV and its intensities of the electron density state is 5.89 *e*/eV. Moreover, the peak coordinates of the 2nd Cu-*d* in PDOS have a bit changes than those of the interior Cu-*d*. Compared with the 2nd and the 3rd curves of the PDOS of Cu-*d* in TiB_2(0001)/Cu(111), 0.09 eV difference has changed from -1.85 eV to -1.76 eV. The curve shape of the PDOS and the coordinates of peaks of the interior Cu atomic layers have few changes above the 3rd Cu-*d*. While for the 7th Cu layer atom, the PDOS curves are obviously different with those of interior Cu atomic layers, because a few electrons un-localized in 15 Å vacuums regions. Therefore, interfacial atoms of TiB_2 in TiB_2(0001)/Cu(111) had effected by two Cu atomic layers. For other TiB_2(0001)/Cu(111) models, similar results could be obtained and which displayed in supplementary information (see as **Fig. S(1) to Fig. S(5),** respectively.)

In general, three TiB_2 and two Cu atomic layers of TiB_2(0001)/Cu(111) (TT-HCP) have confirmed as the interfacial thickness, and the specific values of the interfacial thickness can be expressed by **Eq. (1)**. In **Eq. (1)**, where Δl refers to the interfacial thickness, $l_{TiB_2(z)}$ refers to the z

axis coordinate of the 3rd layer atom of the TiB_2 in TiB_2(0001)/Cu(111) (i.e., for TT-TiB_2/Cu, $l_{TiB_2(z)}$ is z axis coordinate of the 3rd Ti layer atom while for BT-TiB_2/Cu which is z axis coordinate of the 3rd B atomic layer atom) and $l_{Cu(z)}$ is z axis coordinate of the 2nd Cu layer atom. Hence, the interfacial thickness of the TiB_2(0001)/Cu(111) have been predicted and their specific values are displayed in **Table 2**. In **Table 2**, the TT-TiB_2(0001)/Cu(111) interfacial thickness are higher than those of the BT-TiB_2(0001)/Cu(111). For TT-TiB_2(0001)/Cu(111) interfacial models, TT-HCP has the largest interfacial thickness (0.757 nm) contrasting to the smallest interfacial thickness (0.716 nm) of the TT-MT. Nevertheless, the largest interfacial thickness is BT-OT (0.702 nm) and the lowest interfacial thickness is BT-HCP (0.657 nm) for B-terminated TiB_2(0001)/Cu(111) interfacial models. The interfacial thickness of the TT-TiB_2(0001)/Cu(111) models follow the descending order: TT-HCP(0.757 nm)>TT-OT(0.717 nm)>TT-MT(0.716 nm). Similarly, for BT- TiB_2(0001)/Cu(111), the interfacial thickness follow the sequence: BT-OT(0.702 nm) > BT-MT(0.657) =BT-HCP(0.657 nm) from the long to the short. In general, the BT-TiB_2/Cu have the lower interfacial thickness than those of the TT-TiB_2/Cu, which show that the interactions between the B and Cu atom are stronger than those of the Ti and Cu atoms.

3.2 The bond analysis of the TiB_2(0001)/Cu(111)

3.2.1 The bond length and bond populations of theTiB_2 and Cu cell

In order to investigate the electronic structure and bonding state of atoms performed on TiB_2(0001)/Cu(111) interfaces, the Mulliken populations[40] are applied to study the electrons of interfacial atom and bond population of the TiB_2(0001)/Cu(111), TiB_2 cell and Cu cell, respectively. The bond length and populations reflect the character and strength of the bond properties. Therefore, the overlap population could be an objective criterion for bonding state between the two atoms assessing the covalent or ionic nature of a bond[41]. The high value of the bond population indicates the formation of the covalent bond, while the small value implies the ionic interaction maintained between the two atoms. Herein, the ionic character can be measured by the effective ionic valence, namely, the difference between the formal ionic charge and the Mulliken charge on anion species. Nevertheless, if the bond population value is 0 which indicates a perfect ionic bond, if the values greater than zero, which indicate an increasingly levels of covalence involved[42]. Therefore, compared with the changes of the Ti-B, B-B and Cu-Cu bond length at the interfaces of the

TiB_2(0001)/Cu(111), the corresponding bond in TiB_2 and Cu cells also have been calculated initially. The bond length and populations are calculated and displayed in **Fig. 3,** in which it can be noted that the bond length for Ti-B, B-B and Cu-Cu are 2.38 Å, 1.75 Å and 2.57 Å, respectively. Nevertheless, the bond populations are 0.12, 2.39 and 0.04 respective for Ti-B, B-B and Cu-Cu, which indicate that the Cu-Cu bond possess more metallic bond properties, while the B-B bond behave the stronger covalent bond properties, the Ti-B bond either with the metallic bond properties and partial covalent properties. These results have been qualitative confirmed by partial density of the state (PDOS) in previous work, and the mechanism of formation of these bond also have been explained in theoretical study[23].

Table 2. The bond length and bond population (in brackets) calculated for TiB_2 and

Entries	Bond and Population	
	Ti-B	B-B
TiB_2 cell	2.453(0.39)[43]	1.852(2.19)[43]
	2.38(0.12)[this work]	1.75 (2.39)[this work]
TiB_2 in TiB_2/Cu	2.36(0.01) aver. [this work]	1.72(2.86) aver.[this work]

3.2.2 The bond length and bond populations of the TiB_2(0001)/Cu(111)

Since the heterogeneous interfaces have been formed in TiB_2(0001)/Cu(111), in which the bond length of Ti-B, B-B and Cu-Cu at the interfaces are obviously different with those in TiB_2 and Cu cell, respectively. Therefore, the bond length of Ti-B, B-B and Cu-Cu in TiB_2 and Cu cells have been calculated initially to compare with the length changed in TiB_2(0001)/Cu(111). The calculated bond length of Ti-B, B-B and Cu-Cu in TiB_2(0001)/Cu(111) are displayed in **Fig. 3**, and the bond population are displayed inside of the brackets.

In **Table 2.**, it can be noted that our calculated Ti-B (2.38 Å) and B-B (1.75 Å) in TiB_2 cell are similar to those in previous studies, in which Ti-B(2.453 Å) and B-B (1.852) bit higher than our values. Nevertheless, the bond length of Ti-B (2.36 Å aver.) and B-B (1.73 Å aver.) in TiB_2(0001)/Cu(111) are shorter than those in TiB_2 cell (Ti-B is 2.38 Å and B-B is 1.75 Å) in **Fig. 3**. Moreover, for TT-TiB_2(0001)/Cu(111), the bond length of Ti-B(2.33 Å) at the interfaces are shorter than those in its interior and the BT-TiB_2(0001)/Cu(111), which implies that more interaction have been taken placed in TT-TiB_2(0001)/Cu(111). Nevertheless, the bond length of Cu-Cu metallic bond

in TiB_2(0001)/Cu(111) (TT-HCP) are bit shorter than that in Cu cell.

Most importantly, a Ti-Cu bond (2.518 Å) have been detected in TT-HCP and with 0.22 bond population in **Fig. 3(a)**. However, the bond length of Ti-Cu is similar to those of Cu-Cu bond (the average bond length is 2.51 Å) in TT-HCP.

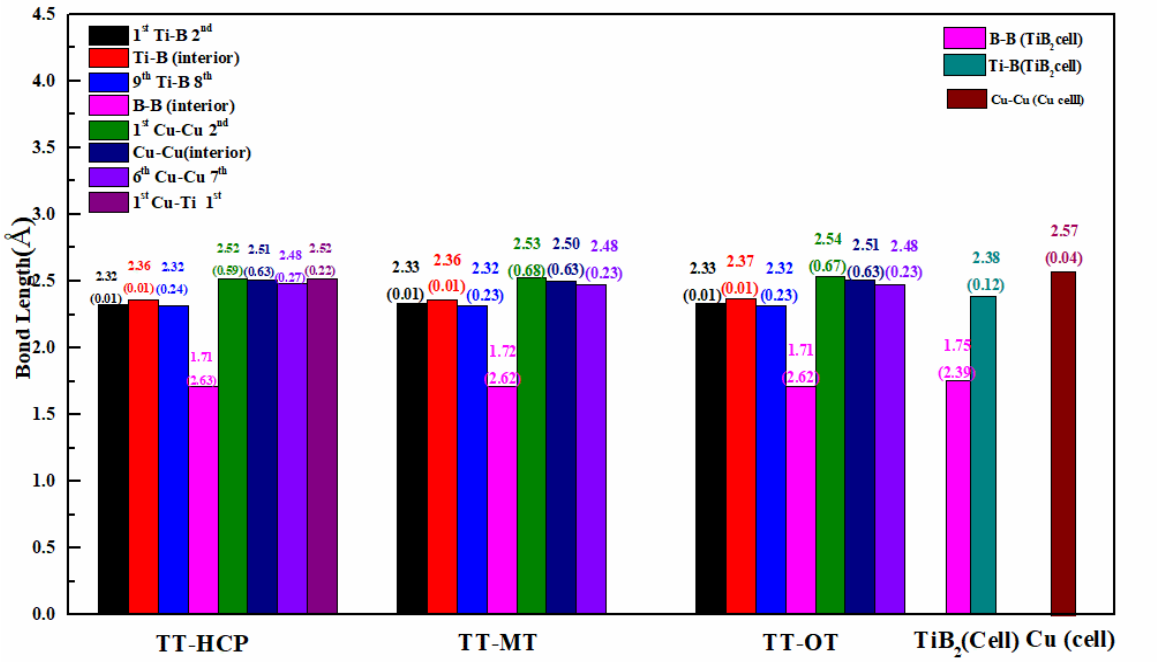

(a)

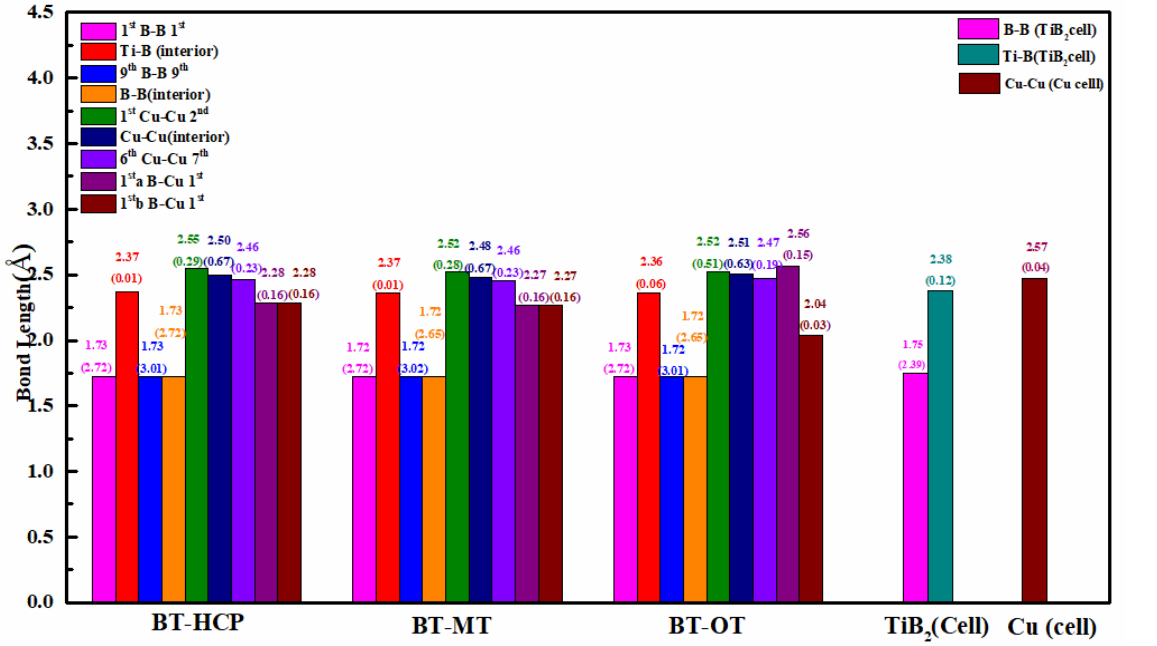

(b)

Fig. 3 The bond length of the TiB_2(0001)/Cu(111): **(a)** Ti-terminated TiB_2(0001)/Cu(111),**(b)** B-terminated TiB_2(0001)/Cu(111).

Since the Ti-Cu bond population is 0.22 which lower than those of the interior and interfacial Cu-Cu bond in TT-HCP, indicating that the Ti-Cu bond possess the metallic bond and partial covalent bond properties. However, there are no Ti-Cu bonds have been detected in TT-OT and TT-MT, which mainly due to the staking ways and spatial location of the interfacial atoms.

Nevertheless, in **Fig. 3 (b)** the Cu-B bond have been detected in all BT-TiB_2(0001)/Cu(111) models, and these bonds are shorter than Ti-B bond in their corresponding models. The average bond length and population of the Cu-B are respective 2.28 Å and 0.13 in three BT-TiB_2(0001)/Cu(111) interfacial models. However, the Cu-B bond length had been detected in chemical compounds is 2.002 Å[44], which is lower than Cu-B bond in BT-TiB_2(0001)/Cu(111).The Ti-B bond is neither performing as the covalent bond nor showing off the purely metallic bond, which is a hybrid bond with most metallic properties and partial covalent properties in TiB_2 cell[43]. Compared with the bond length and the population of the Ti-B bond, the Cu-B bond length and population are similar to Ti-B bond in TiB_2 cell. In addition, the Cu-B has the shortest bond length (2.037 Å) in BT-OT and only with 0.03 bond population, which indicate that Cu-B bond in BT-OT with more metallic property than those of other Cu-B bonds in BT-TiB_2(0001)/Cu(111).

In general, it can be noted that the formed Cu-Ti bond at interface in TT-HCP has the highest interfacial energy but the lowest stability among the TT-TiB_2(0001)/Cu(111). Similarly, the Cu-B bond in BT-OT has the lowest bond length and bond population, which suggest that Ti-Cu bond has the much metallic property and the lowest stability than those of other two BT-TiB_2(0001)/Cu(111). These results are accord well with the results of the W_{ad}, γ_{int}, interfacial distance and interfacial thickness which have been discussed in previous work[23].

3.3 The charge transformation

3.3.1 The charge transformation of Ti and B atoms in TiB_2 cell

The outermost valence of the Ti and the B atoms in TiB_2 are different with the corresponding neutral atoms. For neutral Ti and B atoms, the outermost valence up to their outermost electrons, i.e $3s^2 3p^6 3d^2 4s^2$ are valence electrons for Ti neutral atom which fully counted as 12 *e*, similarly, $2s^2 2p^1$ for the neutral B atom which calculated as 3 *e* in all. Because the bond interactions happened into the TiB_2 between the Ti and the B atoms, the valence electrons of the Ti and the B in TiB2 are various with the corresponding neutral atoms.

The valence electrons for neutral Ti, B and Cu atoms have been displayed in **Table 3,** and they

are 12 *e*, 3 *e* and 11 *e*, respectively. Moreover, the outermost electrons for Ti, B atoms in TiB_2 are different with their corresponding neutral atoms, and they are 10.9 *e* and 3.55 *e* for Ti and B atoms

Table 3. The outermost electrons for the neutral Ti, B and Cu atoms and those of corresponding atoms in TiB_2 and Cu cell.

Entry	Outermost electrons of the atoms (*e*)		
Atoms	Ti	B	Cu
Neutral atom	12	3	11
	10.9[this work]	3.55[this work]	-
TiB_2	10.93[43]	3.54[43]	
	10.82[45]	3.59[45]	

respectively. Therefore, contrasted to the neutral Ti atom, the Ti atom in TiB_2 cell lost 1.1 *e* electrons which are equally shared by the two B atoms surrounded with. Compared with the neutral B atom, each B atom in TiB_2 cell acquiring 0.55 *e*.

3.3.2The charge transformation performed in TiB_2(0001)/Cu(111)

The electron density distribution, electron difference distribution and electron localized function have been discussed for the TiB_2(0001)/Cu(111) in previous work[23], the charge communication performing on interfacial regions of the TiB_2(0001)/Cu(111) have been explicitly confirmed. However, these results only qualitatively study the electron transformation on interfaces of the TiB_2(0001)/Cu(111), while the quantitative study of the charge communication is not specifically discussed. Therefore, the changes of charge difference for each atom performing at the interfaces is still confused, and it is necessary to figure out the charge transformations of the specific atoms undertaking at the interfaces. Therefore, $3d^{10}4s^1$, $3s^23p^63d^24s^2$, and $2s^22p^1$ are applied as the valence electrons for Cu, Ti and B atoms in TiB_2(0001)/Cu(111), respectively. Nevertheless, the specific atoms need to be figured out initially for different models, namely, for TT and BT-TiB_2(0001)/Cu(111) models their specific chemical formula are $Ti_5B_8Cu_7$ and $Ti_4B_{10}Cu_7$, respectively.

Table 4. The calculated total charges for Cu, B and Ti atoms in TiB_2(0001)/Cu(111) (*e*)

Atoms	TT-HCP	TT-MT	TT-OT	BT-HCP	BT-MT	BT-OT
	$Ti_5B_8Cu_7$	$Ti_5B_8Cu_7$	$Ti_5B_8Cu_7$	$Ti_4B_{10}Cu_7$	$Ti_4B_{10}Cu_7$	$Ti_4B_{10}Cu_7$

	Cu-*Thero*.	77	77	77	77	77	77
Cu	Cu-*Cal*.	77.12	77.23	77.22	76.52	76.54	76.64
	Δq_{Cu}	-0.12	-0.23	-0.22	0.48	0.46	0.36
	Ti-*Thero*.	60	60	60	48	48	48
Ti	Ti-Cal.	55.39	55.3	55.29	43.2	43.2	43.16
	Δq_{Ti}	4.61	4.7	4.71	4.8	4.8	4.84
	B-*Thero*.	24	24	24	30	30	30
B	B-*Cal*.	28.48	28.48	28.48	35.32	35.36	35.18
	Δq_{B}	-4.48	-4.48	-4.48	-5.32	-5.36	-5.18

Since the formula of TT-TiB_2(0001)/Cu(111) and BT-TiB_2(0001)/Cu(111) have been determined as $Ti_5B_8Cu_7$ and $Ti_4B_{10}Cu_7$, their theoretical total electrons in outermost layer are respective 161 *e* and 155 *e*. Nevertheless, from the **Table 3**, it can be found that the Ti atom in TiB_2 cell lost 1.10 *e* charges and which are equally shared by two B atoms surrounded. However, due to the environment of the Ti, B and Cu atoms at the TiB_2(0001)/Cu(111) interfaces are different with the Ti and B atoms in TiB_2 cell, the charge transformation more complicated than in those of the TiB_2 cell. Hence, the lost and obtained charges of atoms need to be confirmed initially.

The total charges for all Ti, B and Cu atoms in TiB_2(0001)/Cu(111) have been calculated and then they are followed by subtract the total valence charges of equivalent number of neutral Ti ,B and Cu atoms, so that the specific atoms lost or obtained charges can be finally determined. Moreover, the electrons for each atom in TiB_2(0001)/Cu(111) of six interfacial models have been calculated and which display in **Table S1.** to **Table S6.** The electrons of the ions in TiB_2(0001)/Cu(111) calculated from the **Table S1** to **Table S6**, and then the total results displayed in the **Table 3**. From the **Table 3**, the obtained charges of interfacial Cu and B atoms in TT-TiB_2(0001)/Cu(111) are mostly equivalent to the lost charges of the interfacial Ti atom. While for BT-TiB_2(0001)/Cu(111) interfaces, the acquired charges of the interfacial B atoms from the Cu and Ti atoms, respectively. Though the change of the charges is different for different interfaces, the number of the obtained charges are equivalent to the lost charges, and which can be expressed by **Eq. (2)** and **Eq. (3)**:

$$\Delta \mathrm{q}_{Ti} = \Delta q_{Cu} + \Delta q_{B} \quad \textbf{(2)}$$

$$\Delta q_B = \Delta q_{Cu} + \Delta q_{Ti} \quad \textbf{(3)}$$

In the **Eq.(2)** and the **Eq.(3)**, where Δq_{Ti}, Δq_{Cu} and Δq_B refer to the lost or the obtained charges for Ti, Cu and B atoms respectively. Moreover, the positive value of the Δq means the loss of charges while the negative values indicate the obtaining of the charges. Compared with the Δq values in **Table 4**, Cu atoms obtained the charges various from 0.12 *e* (TT-HCP) to 0.23 *e* (TT-MT) in TT-TiB_2(0001)/Cu(111), while Ti atoms lost charges are various from 4.61*e* (TT-HCP) to 4.71 *e* (TT-OT), the same charge obtained (4.48 *e*) for B atoms in all TiB_2(0001)/Cu(111) interfacial models. However, for BT-TiB_2(0001)/Cu(111) interfacial models, the interfacial Cu atoms lose charges various from 0.48 *e* (BT-HCP) to 0.36 *e* (BT-OT) while Ti atoms lost charges different from 5.32 *e* (BT-HCP) to 5.18 *e* (BT-OT), and B atoms acquire 4.8 *e* (BT-HCP), 4.8 *e* (BT-MT) and 4.84 *e* (BT-OT) charges, respectively. Therefore, according to the **Eq. (2)** and **Eq. (3)**, it can be found that the lost charges are basically equal to the obtained charges, and with no more than 0.03 *e* difference.

Since the charge communication is mostly performed at the interfacial layers of the heterogeneous interfaces, however, the interfacial thickness in our previous study confirmed that the charge transformation is mainly performed on three TiB_2 atomic layer and two Cu atomic layer, respectively. Therefore, the five interfacial layer atoms are chosen to study the charge transformation carried on interfaces. In order to determine the layers of the atoms in TiB_2(0001)/Cu(111), the 1st Ti, the 2nd B, the 3rd Ti, the 1st Cu and the 2nd Cu five layer atoms have been chosen for TT-TiB_2(0001)/Cu(111) and the 1st B, the 2nd Ti, the 3rd B, the 1st Cu and the 2nd Cu five layer atoms have been selected for BT-TiB_2(0001)/Cu(111) in **Table 5,** for further investigation of the charge transformation. The 2nd layer B atoms not only effected by the 1st layer Ti atom but also influenced by the 3rd layer Ti atom in TiB_2(0001)/Cu(111), and it is similarly for the 2nd Ti layer atoms which influenced by both the 1st and the 3rd layer B atoms in BT- TiB_2(0001)/Cu(111). Herein, the **Eq. (2)** and the **Eq. (3)** can be further expressed as the **Eq. (4)** and the **Eq. (5)** by considering the electronic influence of the fifth layer atoms.

$$\Delta \mathbf{q}_{\boldsymbol{Ti1^{st}}} = \Delta \mathbf{q}_{\boldsymbol{Cu1^{st}}} + \Delta \mathbf{q}_{\boldsymbol{Cu2^{nd}}} + \Delta \mathbf{q}_{\boldsymbol{B2^{nd}a}} + \Delta \mathbf{q}_{\boldsymbol{B2^{nd}b}} - \frac{\Delta \mathbf{q}_{\boldsymbol{Ti3^{rd}}}}{2} \quad \textbf{(4)}$$

$$\Delta \mathbf{q}_{\boldsymbol{B1^{st}a}} = \Delta \mathbf{q}_{\boldsymbol{Ti2^{nd}}} + \frac{(\Delta \mathbf{q}_{\boldsymbol{B3^{rd}a}} + \Delta \boldsymbol{q}_{\boldsymbol{B3^{rd}b}})}{2} + \Delta \boldsymbol{q}_{\boldsymbol{Cu1^{st}}} + \Delta \boldsymbol{q}_{\boldsymbol{Cu2^{nd}}} - \Delta \boldsymbol{q}_{\boldsymbol{B1^{st}b}} \quad \textbf{(5)}$$

Based on the specific values in **Table 4**, the interfacial charge transformations are carried out via

the **Eq. (4)** and the **Eq. (5)**, and the calculated lost charges mostly equal to the obtained charges within no more than 0.02 *e* difference. Taking TT-HCP for instance, however, the loss of the charge of the

Table 5. The charge difference for the interfacial Ti, B and Cu atoms in TiB_2(0001)/Cu(111) (*e*)

	atoms	TT-HCP $Ti_5B_8Cu_7$	TT-MT $Ti_5B_8Cu_7$	TT-OT $Ti_5B_8Cu_7$	BT-HCP $Ti_4B_{10}Cu_7$	BT-MT $Ti_4B_{10}Cu_7$	BT-OT $Ti_4B_{10}Cu_7$
Ti	1^{st} Ti	11.28	11.17	11.17	-	-	-
	$\Delta q_{1^{st}Ti}$	0.72	0.83	0.83	-	-	-
	2^{nd} B	7.13	7.13	7.13	-	-	-
	$\Delta q_{2^{nd}B}$	-1.13	-1.13	-1.13	-	-	-
	3^{rd} Ti	10.89	10.89	10.89	-	-	-
	$\Delta q_{3^{rd}Ti}$	1.11	1.11	1.11	-	-	-
B	1^{st} B	-	-	-	7.10	7.10	6.98
	$\Delta q_{1^{st}B}$	-	-	-	-1.10	-1.10	-0.98
	2^{nd} Ti	-	-	-	10.84	10.84	10.8
	$\Delta q_{2^{nd}Ti}$	-	-	-	1.16	1.16	1.21
	3^{rd} B	-	-	-	7.12	7.12	7.12
	$\Delta q_{3^{rd}B}$	-	-	-	-1.12	-1.12	-1.12
Cu	1^{st} Cu	11.10	11.22	11.22	10.64	10.64	10.74
layer	$\Delta q_{1^{st}Cu}$	-0.1	-0.22	-0.22	0.37	0.37	0.26
	2^{nd} Cu	11.03	11.02	11.01	10.9	10.9	10.94
	$\Delta q_{2^{nd}Cu}$	-0.03	-0.02	-0.01	0.11	0.11	0.06

1^{st} Ti atom is 0.72 *e* contrasting to the obtained 0.71 *e* of the Cu and the B atoms, and the difference between the obtained and the lost charges is only 0.01 *e*. Nevertheless, for other TT-TiB_2(0001)/Cu(111) interfacial models, the loss of the charges of the interfacial Ti atoms are mostly equal to the obtained atoms. Moreover, the 1^{st} layer two B atoms of the BT-OT obtains the lowest charge (0.98 *e*) among three BT-TiB_2(0001)/Cu(111) interfacial models and for other two BT-HCP and BT-MT, the first layer of the two B atoms obtained the same charges as 1.10 *e*. Nevertheless, there are less charge transformations performed on TT-HCP and BT-OT interfaces rather than their

corresponding atom-terminated TiB_2(0001)/Cu(111), which reveal that these two interfacial models with less interfacial interactions than their corresponding atom-terminated TiB_2(0001)/Cu(111). Because the interfacial bonding and charge transformation are the key parameters for interfacial stability of the TiB_2(0001)/Cu(111), the change of the electrons belonged to the orbit leading the hybridization of the orbitals . Therefore, the electrons belonged to $3d^{10}4s^1$, $2p^63d^24s^2$ and $2s^22p^1$ for Cu, Ti and B atoms in TiB_2(0001)/Cu(111) need to be analyzed to investigate specific changes of the oribits, respectively.

3.2.3 Orbital electrons transformation of the interfacial atoms of the TiB_2/Cu

Since the TiB_2 is an ionic crystal, which contains two types of the bond, i.e., the δ bond and the π bond. The δ bond are formed due to the sp^2 hybridization happened during the two B^- anionic acquiring the electrons. However, the $2p_z$ orbital of the two B^- anionic not involving the hybridization and leading to the combination of the localized π bond[43]. According to the **Table 6**, the electrons belonged to B-*s*, Ti-*s* and Cu-*s* orbits have apparently changed comparing with their corresponding neutral orbitals' electrons for TiB_2(0001)/Cu(111). For instance, the electrons belonged to the B-*s* orbit in TiB_2 and TiB_2/Cu are less than 2 *e*, which implied that they loss about 1.1 *e*, 1.088 *e* and 1.088 *e* electrons and keeping 0.9 *e*, 0.912 *e* and 0.912 *e* remained for TT-TiB_2/Cu, BT-TiB_2/Cu and TiB_2, respectively. Therefore, the charge transformation of the B-2*s* is mainly performed due to the hybridization of the electrons belonged to the 2*s* and 2*p* orbits. Similarly, the electrons in Ti-*s*, Ti-*p*, Ti-*d*, Cu-*s*, Cu-*p* and Cu-*d* orbits are also different with their corresponding neutral orbital electrons in **Table 6**. Taking TT-TiB_2(0001)/Cu(111) for instance, the electrons of the Ti-*s* orbit are various form 0.089 *e* (TT-HCP) to 0.057 *e* (TT-OT) higher than those of the Ti-*s* -0.13 *e* in TiB_2, which reveal that the later are much hybrid than electrons in Ti-*s* orbit of the TiB_2(0001)/Cu(111). Moreover, it further indicates that the partial charges of Ti-4*s* and Cu-4*s* orbitals transferred into their 3*d* and 4*p* orbits. In terms of the overlapping electronic cloud orbits, strong bonding covalent between the B atoms corresponding to their larger electronic cloud orbital numbers. However, for the Ti-B, the Cu-B and the Ti-Cu (only in TT-HCP) bonds, the overlapping electronic cloud orbitals are relatively smaller and more inclined to be interacted of the ions. In comparison with the electrons in Ti-*s*, Ti-*p* and Cu-*d* orbits of the TT and BT-TiB_2(0001)/Cu(111), the electrons in Ti-*s* orbit of the BT-TiB_2(0001)/Cu(111) mainly transferred to other orbit rather than the electrons in Ti-*s* orbit of TT-TiB_2(0001)/Cu(111) still within partial electrons remained.

Moreover, the electrons in Ti-2*p* and Cu-3*d* orbits of the BT-TiB_2(0001)/Cu(111) are more

Table 6 The electrons in *s*, *p*, *d* orbitals belonged to B, Ti and Cu atoms at the TiB_2/Cu interfaces, TiB_2 cell and Cu respectively. For TT-TiB_2/Cu, Ti and B refers to the 1st Ti and 2nd B layer atoms

atoms	orbital	TT-HCP	TT-MT	TT-OT	BT-HCP	BT-MT	BT-OT	TiB_2 cell	Cu cell
B	s	0.896	0.899	0.899	0.912	0.912	0.912	0.912	/
	p_x	0.881	0.880	0.879	0.904	0.904	0.854	0.873	/
	p_y	0.881	0.880	0.879	0.904	0.904	0.854	0.873	/
	p_z	0.914	0.907	0.911	0.930	0.930	0.750	0.893	/
Ti	s	0.089	0.060	0.057	-0.132	-0.136	-0.132	-0.130	/
	d_z^2	0.538	0.463	0.461	0.472	0.472	0.470	0.505	/
	d_{zy}	0.456	0.502	0.502	0.538	0.540	0.542	0.541	/
	d_{zx}	0.456	0.506	0.502	0.538	0.538	0.542	0.541	/
	$d_{x^2-y^2}$	0.612	0.593	0.599	0.594	0.594	0.580	0.576	/
	d_{xy}	0.612	0.595	0.599	0.594	0.594	0.580	0.576	/
	p_x	0.222	0.196	0.195	0.144	0.142	0.150	0.148	/
	p_y	0.222	0.196	0.195	0.144	0.144	0.150	0.148	/
	p_z	0.057	0.032	0.041	-0.098	-0.100	-0.126	-0.041	/
Cu	d_z^2	1.918	1.940	1.942	1.972	1.972	1.894	/	9.76 (total)
	d_{zy}	1.939	1.927	1.931	1.902	1.904	1.938	/	
	d_{zx}	1.939	1.926	1.931	1.902	1.902	1.938	/	
	$d_{x^2-y^2}$	1.963	1.952	1.946	1.934	1.936	1.960	/	
	d_{xy}	1.963	1.951	1.946	1.934	1.934	1.960	/	
	s	0.716	0.793	0.781	0.504	0.504	0.632	/	1.05 (total)
	p_x	0.229	0.231	0.227	0.160	0.158	0.144	/	
	p_y	0.229	0.231	0.227	0.160	0.160	0.144	/	
	p_z	0.201	0.271	0.290	0.162	0.164	0.138	/	

hybridized than those of the TT-TiB_2(0001)/Cu(111). In **Table 6,** it can be found that the charges in $2p_x$ orbits equal to those in $2p_y$ orbits of Ti, B Cu atoms. For Ti and Cu atoms, the charges in $3d_{xy}$ equal to those in $3d_{x^2-y^2}$, and it is similar to the charges in $3d_{zx}$, $3d_{zy}$ orbits of Cu and Ti atoms in

TiB_2(0001)/Cu(111). Compared with the charges in orbits, the charges in B-s and B-*p* orbits of the TiB_2/Cu are higher than those in TiB_2 (excepting for the charges in B-*p*), which show that electrons of the B in TiB_2 cell more hybridized than those at the interfaces in TiB_2(0001)/Cu(111). Nevertheless, The charges in d_{zy} and d_{zx} orbits of the Cu and Ti of the TiB_2(0001)/Cu(111) are lower than corresponding of those in TiB_2 cells. The charges in $d_{x^2-y^2}$ and d_{xy} orbits of the Ti atoms of the TiB_2(0001)/Cu(111) are also higher than those of the Ti atoms in TiB_2 cell.

In general, based on above these hybridizations of the electron orbitals lead more covalent properties of the TT-TiB_2(0001)/Cu(111) than those of the BT-TiB_2(0001)/Cu(111), which indicate that BT-TiB_2(0001)/Cu(111) are more stable than TT-TiB_2(0001)/Cu(111).

4 Conclusion

In this work, the charge transformation of the interfacial atoms for TiB_2/Cu were studies via the first principles. The relationship between the charge transformation and stabilities of the interfaces indicated that the bonding state and ways determined the stability of the heterogeneous interfaces, and main results can be generalized as below:

(1) The interfacial thickness layers have been calculated for TiB_2/Cu composites via the PDOS. The interfacial thickness layers of the TT-TiB_2/Cu are higher than 0.715 nm, while those of the BT-TiB_2/Cu are lower than 0.715 nm.

(2) The metallic bond Ti-Cu have been detected only in TT-HCP with the bond length and population are 2.518 Å and 0.22, respectively. However, the B-Cu ionic bond have been discovered in all BT-TiB2/Cu interfacial models, and the average bond length is 2.28 Å and the bond population is 0.13.

(3) The Ti-Cu and B-Cu bond have been confirmed due to the charge hybridization of the *d*-*p* orbit, which further verified the metallic and ion bonds formed by interfacial atoms of the TiB_2(0001)/Cu(111).

Data availability

The datasets generated during and analyzed during the current study are available from the corresponding author on reasonable request.

Code availability

N/A.

Acknowledgments

The authors appreciate the financial support from the Guangdong Academy of Science (Grant

No. 2021GDASYL-20210103099), (Grant No. 2021GDASYL-20210102002), (Grant No. 2020GDASYL-20200101001) Guangdong Province Key Area R and D Program (2020B0101340004, 2020B0301030006) and Nanchang University (9140/06301549).

Corresponding authors:

Yao Shu, email:shuyao@gdinm.com; Shaowen Zhang, email: swzhang@bit.edu.cn; Kaihong Zheng, email:zhengkaihong@gdinm.com

Ethics declarations

Conflict of Interest

The authors declare that they have no conflict of interest.

Author information

Affiliations

[a]***Institute of New Materials, Guangdong Academy of Sciences, Guangzhou, 510651, Guangdong, P.R.China***

[b]***Guangdong Provincial Key Laboratory of Metal Toughening Technology and Application, Guangzhou, 510651, Guangdong, P.R.China.***

Yao Shu, Juan Wang, Xiongyong Nan, Xing Luo, Jiazhen He, Cuicui Yin, Kaihong Zheng, Fuxing Yin, Fusheng Pan.

[c] ***School of materials Science and Engineering, Nanchang University, Nanchang, Jiangxi, 330031, P.R.China.***

Fei Gao

[d] ***School of Chemistry and Chemical Engineering, Key Laboratory of Cluster Science of Ministry of Education, Beijing Institute of Technology, South Zhongguancun Street #5, Haidian District, Beijing 100081, P.R.China.***

Shaowen Zhang

Authors' contributions:

Yao Shu worked on calculation and writing draft of the manuscript; Juan Wang and Kaihong Zheng were mainly responsible for supervisions during this work; Yongnan Xiong and Xing Luo undertook the visualization and investigation. Jiazhen He and Cuicui Yin were responsible for data curation and formal analysis. Fei Gao prepared for draft and investigation. Shaowen Zhang wrote-reviewed and edited for this work; Fuxing Yin and Fusheng Pan were taken financial support for this work.

Reference

1 Jamwal A, Mittal P, Agrawal R. (2020) Towards sustainable copper matrix composites: Manufacturing routes with structural, mechanical, electrical and corrosion behavior. J. Compos Mater DOI:10.1177/0021998319900655

2 Sridhar MMJ, Ravichandran M, Meignanamoorthy M. (2020) Influence of different reinforcements on properties of copper matrix composites: A review 2283, 020129. AIP Conference Proceedings 2283, 020129. DOI: 10.1063/5.0029257

3 Fabritsiev SA, Pokrovsky AS, Ostrovsky SE. (2004) Effect of the irradiation–annealing–irradiation cycle on the mechanical properties of pure copper and copper alloy.J Nucl Mater, 324,23-32.DOI: 10.1016/j.jnucmat.2003.09.004

4 Islamgaliev RK, Sitdikov, VD, Nesterov KM, Pankratov DL. (2014) Structure and Crystallographic Texture in the Cu-Cr-Ag Alloy Subjected to Severe Plastic Deformation. Rev. Adv. Mater. Sci 39 61-68. DOI: 10.4028/www.scientific.net/AMM.872.61

5 Tschopp, MA, Murdoch HA, Kecsjes LJ, Darling KA. (2014) “Bulk” Nanocrystalline Metals: Review of the Current State of the Art and Future Opportunities for Copper and Copper Alloys. The Minerals, Metals & Materials Society(TMS), DOI: 10.1007/s11837-014-0978-z.

6 Tomioka Y, Miyake J. (1995) A copper alloy development for leadframe, Proceedings of 1995 Japan International Electronic Manufacturing Technology Symposium,433-436. DOI: 10.1109/IEMT.1995.541079.

7 Jadhav SD, Dhekne PP, Dadbakhsh S, Kruth JP, Humbeeck JV, Vanmeensel K. (2020) Surface Modified Copper Alloy Powder for Reliable Laser-based Additive Manufacturing. Addit Manuf 35 101418. DOI:10.1016/j.addma.2020.101418

8 Qin YQ, Tian Y, Peng YQ, (2020) Research status and development trend of preparation technology of ceramic particle dispersion strengthened copper-matrix composites. J Alloy Compd. 848 156475. DOI: 10.1016/j.jallcom.2020.156475

9 Jamwal A, Mittal P, Agrawal, R (2020) Towards sustainable copper matrix composites: Manufacturing routes with structural, mechanical, electrical and corrosion behavior. J Compos Mater (0) 1-15. DOI:10.1177/0021998319900655

10 Zhang XH, Zhang Y, Tian BH (2019) Review of nano-phase effects in high strength and

conductivity copper alloys. Nanotechnol Rev 8 383-395. DOI: 10.1515/ntrev-2019-0034.

11 Uzun M, Usca UA (2018) Effect of Cr particulate reinforcements in different ratios on wear performance and mechanical properties of Cu matrix composites. Journal of the Brazilian Society of Mechanical Sciences and Engineering. 40 197. DOI:10.1007/s40430-018-1130-8.

12 Bai H, Ma NN, Lang J, Jin Y (2013) Thermo-physical properties of boron carbide reinforced copper composites fabricated by electroless deposition process. Mater Design DOI:10.1016/j.matdes.2012.09.053.

13 Bagheri GH A. (2016) The effect of reinforcement percentages on properties of copper matrix composites reinforced with TiC particles. J Alloy Compd. 676 120-126. DOI: 10.1016/j.jallcom.2016.03.085.

14 Yusoff M, Othman R, Hussain Z (2011) Mechanical alloying and sintering of nanostructured tungsten carbide-reinforced copper composite and its characterization. Mater Design 32 3293-3298. DOI: 10.1016/j.matdes.2011.02.025.

15 Shehata F, Fathy A, Abdelhameed M, Moustafa SF. (2009) Preparation and properties of Al_2O_3 nanoparticle reinforced copper matrix composites by in situ processing. Mater Design 30 2756-2762. DOI: 10.1016/j.matdes.2008.10.005.

16 Fathy A, Elkady O, Abu-Oqail A. (2017) Production and properties of Cu-ZrO_2 nanocomposites. J Compos Mater (0) 1-11. DOI: 10.1177/0021998317726148

17 Yin JW, Yao DX, Hu HL, Xia YF, Zuo KH, Zeng YP. (2014) Improved mechanical properties of Cu matrix composites reinforced with β-Si3N4 whiskers. 607 287-293. DOI: /10.1016/j.msea.2014.04.021.

18 Ramírez-Vinasco D, León-Patiño CA, Aguilar-Reyes EA, Pech-Canul MI. (2020) Preparation of AlN-Cu composite powders by electroless plating of controlled oxidized nitride particles to prevent degradation by hydrolysis. 31 937- 946. DOI: 10.1016/j.apt.2019.12.014.

19 Zhao GL, Smith R, Raynolds J (1996) First-principles study of the α-Al_2O_3(0001)/Cu(111) Interface, Interface Sci 3 (1996) 289-302. DOI: 10.1007/BF00194707.

20 Zhang K, Zhan YZ. (2019) Adhesion strength and stability of Cu(111)/TiC(111) interface in composite coatings by first principles study. Vacuum 165 215-222. DOI: 10.1016/j.vacuum.2019.04.028.

21 Wu ZX, Pang MJ, Zhan YZ, Shu S, Xiong L, Li ZH. (2021) The bonding characteristics of the Cu(111)/WC(0001) interface: An insight from first-principle calculations. Vacuum 191 110218. DOI: 10.1016/j.vacuum.2021.110218.

22 Pang XZ, Yang JB, Pang MJ, He JX (2019) Theoretical understanding of atomic and electronic structures of the ZrC(111)/Cu(111) interface. J Alloy Compond. 791 431-437. DOI: 10.1016/j.jallcom.2019.03.276.

23 Shu Y, Xiong YN, Luo X (2021) Adhesion strength, stability and electronic properties of TiB_2 reinforced copper matrix composites: A first principles study. Physica B: Condensed Matter. 625c 413457. DOI: 10.1016/j.physb.2021.413457.

24 Liu Y, Li JY, Tschirhart TY (2017) Connecting Biology to Electronics: Molecular Communication via Redox Modality. Adv Healthcare Mater 6(24) 1700789. DOI: 10.1002/adhm.201700789.

25 Bakulin AA, Lovrincic R, Yu X, Selig O, (2015) Mode-selective vibrational modulation of charge transport in organic electronic devices. Nature Commun. 6 (1) DOI: 10.1038/ncomms8880.

26 Sakai K, Okada Y, Uemura T, (2016) The emergence of charge coherence in soft molecular organic semiconductors via the suppression of thermal fluctuations. NPG Asia Materials 8 e252. DOI: 10.1038/am201630.

27 Shu Y, Lei H, Tan YN (2014) Tuning the electronic coupling in Mo_2-Mo_2 systems by variation of the coordinating atoms of the bridging ligands. Dalton Tans. 43(39) 14756-14765. DOI: 10.1039/c4dt00786g.

28 Kang S, Jeong YK, Mhin S, Ryu JH (2021) Pulsed Laser Confinement of Single Atomic Catalysts on Carbon Nanotube Matrix for Enhanced Oxygen Evolution Reaction. ACS Nano, 15(3) 4416-4428. DOI: 10.1021/acsnano.0c08135.

29 Kumari R, Ahlawat N, Agarwal A, Sanghi S, Sindhu M. (2017) tructural transformation and investigation of dielectric properties of Ca substituted $(Na_{0.5}Bi_{0.5})_{0.95}$−x$Ba_{0.05}CaxTiO_3$ ceramics. J Aolly Compnd 695 3282-3289. DOI: 10.1016/j.jallcom.2016.11.200.

30 Filho A, Silva RV, Cardpsp WS (2014) Effect of niobium in the phase transformation and corrosion resistance of one austenitic-ferritic stainless steel. Material Research 17(4) 801-806. DOI: 10.1590/1516-1439.190113.

31 Xu S, Lin HJ, Lin X (2021) Intercalating ultrathin polymer interim layer for charge transfer cascade towards solar-powered selective organic transformation. Journal of Catalysis 399 150-161.DOI: 10.1016/j.jcat.2021.05.005.

32 Xiong HH, Jiang PG, Du Z, et al. (2017) Investigation on adhesion strength, stability and electronic properties of Ti/TiB_2 interface by first-principles (in Chinese). Chin Sci Bull, 62: 1655-1661. DOI: 10.1360/N972017-00120.

33 Han YF, Dai YB, Shu D, Wang J, Sun BD (2006) First-principles study of TiB_2(0001) surfaces. J. Phys.: Condens. Matter 18 4197-4205. DOI: 10.1088/0953-8984/18/17/008.

34 Appelbaum JA, Hamann DR, (1978) Electronic structure of the Cu (111) surface. Solid state Commun 27 881-883. DOI: 10.1016/0038-1098(78)90197-7.

35 Segall MD, Philip JD, Lindan, Probert, MJ. (2002) First-principles simulation: ideas, illustrations and the CASTEP code, J. Phys.: Condens. Matter 14 2717-2744. DOI: 10.1088/0953-8984/14/11/301.

36 Clark SJ, Segall MD, Pickard C J, et al. (2005) First principles methods using CASTEP, Zeitschrift für Kristallographie 220 567-570. DOI: 10.1524/zkri.220.5.567.65075.

37 Perdew JP, Burke K, Wang Y, et al. (1996) Generalized gradient approximation for the exchange-correlation hole of a many-electron system, Phys. Rev. B 54 16533-16539. DOI: 10.1103/PhysRevB.54.16533.

38 Monkhorst HJ, Pack JD (1976) Special points for Brillouin-zone integrations, Phys. Rev. B 13 5188-5192. DOI: 10.1103/PhysRevB.13.5188.

39 Fischer TH, Almlof J. (1992) General methods for geometry and wave function optimization, J. Phys. Chem 96 9768-9774. DOI: 10.1021/j100203a036.

40 Reed AE, Weinstock RB, Weinhold F. (1985) Natural population analysis. J.Chem.Phys. 83 735. DOI: 10.1063/1.449486.

41 Wu YL, Zhang L, Liu Y, Qu YP. (2018) Adsorption mechanisms of metal ions on the potassium dihydrogen phosphate (100) surface: A density functional theory-based investigation. 522 256-263.

DOI: 10.1016/j.jcis.2018.03.073.

42 Segall MD, Shah R, Pickard CJ. (1996) Population analysis of plane-wave electronic structure calculations of bulk materials, Physical Review B 54 (23) 317-320. DOI: 10.1103/PhysRevB.54.16317.

43 Yu L, Zhang YJ, Kang XA, Jiang YL (2019) First Principles Calculation of the Electronic Structure, Optical and Lattice Kinetic Properties of TiB_2 Applied Physics 9(5) 259-268. DOI: 10.12677/app.2019.95031.

44 Laitat DS, Müller P, Sadighi JP. (2005) Efficient Homogeneous Catalysis in the Reduction of CO_2 to CO, J. Am. Chem. Soc 127 17196-17197.DOI: 10.1021/ja0566679.

45 Yan HY, Wei Q, Chang SM, Guo P. (2011) A first-principle calculation of structural, mechanical and electronic properties of titanium borides. 21 1627-1633. DOI: 10.1016/S1003-6326(11)60906-0.

Supplementary Files

This is a list of supplementary files associated with this preprint. Click to download.

- supportinginformation2.docx
- Graphiccontent1.png